Double helical and monomeric Ag(I) and Zn(II) complexes of 1,2-cyclohexanediyl-bis(iminophenanthridine) ligands

Valeria Amendola,[a] Yuri Diaz Fernandez,[b] Carlo Mangano,[a] Marco Montalti,[c] Piersandro Pallavicini,*[a] Luca Prodi,*[b] Nelsi Zaccheroni[c] and Michele Zema[d]

[a] *Dipartimento di Chimica Generale, Università di Pavia, v. Taramelli 12, 27100 Pavia, Italy.* *E-mail: psp@unipv.it; Fax: xx.39.0382.528544; Tel: xx.39.0382.507329*
[b] *Instituto Superior de Ciencias y de Tecnologias Nucleares, Ave. Salvador Allende y Luaces, Quinta de los Molinos, Plaza de la Ravolucion, Habana, Cuba*
[c] *Dipartimento di Chimica "G. Ciamician", Università degli Studi di Bologna, v. Selmi 6, 40126 Bologna, Italy. E-mail: lprodi@ciam.unibo.it; Fax: xx.39.051.2099456; Tel: xx.39.051.2099481*
[d] *Centro Grandi Strumenti, Università di Pavia, via Bassi, 9, I27100 Pavia, Italy*

The tetradentate ligands **tcp** and **ccp**, made of two bidentate iminophenanthridine halves, separated, respectively, by *trans*- and *cis*-cyclohexanediyl spacers, have been studied in acetonitrile as regards their ability of coordinating the d^{10} cations Ag^+ and Zn^{2+}. Spectrophotometric and spectrofluorimetric titrations revealed the tendency to form 1 : 2 and 2 : 2 metal–ligand complexes for Ag^+, when metal–ligand molar ratios lower than 1 : 1 are chosen. Determination of the formation constants of the 1 : 2 and 2 : 2 complex species demontrate that at metal–ligand molar ratio = 1 : 1 the preferred species are the helicates $[Ag^I_2(\textbf{tcp})_2]^{2+}$ and $[Ag^I(\textbf{ccp})_2]^{2+}$, whose nature was been further supported by ^1H NMR and ESI-MS spectra. The crystal and molecular structure of $[Ag_2(\textbf{ccp})_2](CF_3SO_3)$-$(Et_2O)$ has also been determined by X-ray diffraction, confirming the double helical nature of the molecular cation. The same ligands tend to form 1 : 2 and 1 : 1 metal–ligand complexes with Zn^{2+} in acetonitrile, at molar ratios lower than 1 : 1. However, only the monomeric $[Zn(\textbf{tcp})]^{2+}$ and $[Zn(\textbf{ccp})]^{2+}$ complexes are formed at 1 : 1 stoichiometry, as indicated by calculation of formation constants, and by ^1H NMR and ESI-MS spectra. The luminescent properties of the ligands have been also studied, which are connected to the presence of the luminescent phenanthridine heterocycle. In the free ligands, intramolecular excimer formation between the two phenanthridine halves of the molecule occurs. Complexation of the ligands with Ag^+ affords non-luminescent helicates, while the monomeric complexes obtained with Zn^{2+} are strongly luminescent.

Introduction

Bis-bidentate ligands of the bis(iminoheterocycle) type may be easily prepared from a diamine molecule and two equivalents of the chosen heterocyclic aldehyde. Double helical metal complexes are then obtained by using metal cations preferring tetrahedral coordination, provided that the fragment separating the two bidentate units is rigid and short enough to prevent the wrapping of a single ligand around a single metal cation according to a tetrahedral geometry. Some papers have appeared regarding ligands of this kind featuring heterocycles of the N-donor type which range from thiazole to phenanthridine. The employed spacers were of the 1,2-ethanediyl, *trans*-1,2-cyclohexanediyl and *cis*-1,2-cyclohexanediyl type and double helical complexes were obtained with Cu(I).[1] Noticeably, the same ligands form 1 : 1 monomeric complexes with Cu(II), due to the coordinative preferences of this d^9 cation, which prefers to be five- or six-coordinated, with tetradentate ligands arranging in a more or less distorted square disposition around the cation, and with one or two solvent molecules completing the coordination sphere. Moreover, it is possible to reversibly switch electrochemically between Cu(I) helical dimers and Cu(II) monomers, with electrochemical profiles displaying hysteresis.[1] On the other hand, very few papers have appeared with this kind of ligands and metal cations different from copper. Ag(I) and Zn(II) are d^{10} cations, *i.e.* they are isoelectronic with Cu(I). Ag(I) in particular has been exstensively employed as a "tetrahedral cation" in the formation of classical polypyridine[2a–c] and imino-pyridine helicates,[2d,e] while the harder Zn(II) cation, preferring coordination numbers ranging

from six to four,[3a] has been more rarely employed in the formation of double or triple helical complexes.[3b,c] Despite of the expected similar behaviour of Ag(I) with respect to Cu(I), so far only one paper has appeared in which its double helical complex with a bis(iminoheterocycle) ligand featuring a *cis*-1,2-cyclohexanediyl spacer was studied (in that case, an Ag^+ double helical complex was obtained, with pyridine as the heterocycle).[4] In this paper, we describe the coordinative behaviour of ligands **tcp** and **ccp** with Ag^+ and Zn^{2+}. The two ligands contain the *trans*-1,2-cyclohexanediyl or *cis*-1,2-cyclohexanediyl spacer, respectively, while the heterocycle is phenanthridine. The expected double helical complexes are obtained with the "tetrahedral" Ag^+ cation, while monomeric complexes are obtained in the case of the Zn^{2+} cation, which in this case behaves similarly to Cu^{2+}. The solution and solid state structures of the complexes are discussed on the basis of X-ray diffraction, ^1H NMR, spectrophotometric titrations and electron-spray mass measurements. Moreover, these ligands show interesting luminescent properties due to the chromophoric phenanthridine fragment and we have investigated the variations of their photopshysical properties upon complexation with Zn^{2+}, Ag^+ and Cu^+.

Experimental

Syntheses

Ligands **tcp** (*R,R* isomer) and **ccp** were synthesized as already described.[1d] Phenanthridine aldehyde was prepared according to literature methods.[5]

tcp
(trans, RR form)

ccp
(cis, meso form)

cp
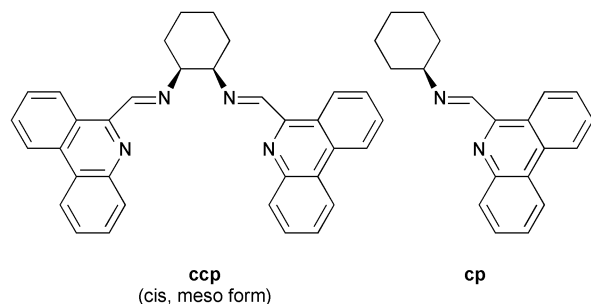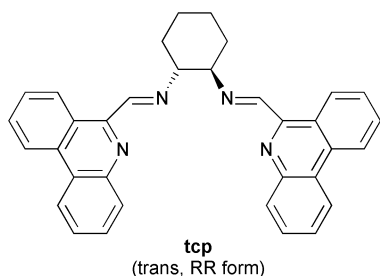
Cyclohexyliminophenanthridine (cp)

0.17 g (1.5 mmol) of commercial (Aldrich) cyclohexylamine and 0.31 g (1.5 mmol) phenanthridine aldehyde were dissolved in 20 ml CH_2Cl_2 and stirred overnight at room temperature. An excess of anhydrous $MgSO_4$ was then added to remove the produced water. The mixture was then filtered, the solvent removed on a rotary evaporator and the obtained product treated with *n*-hexane to obtain **cp** as a rough white solid. Yield: 92%. Anal. Calc. for $C_{20}H_{20}N_2$: C 83.30, H 6.99, N 9.71%. Found: C 83.10, H 7.09, N 9.64%. ^{1}H NMR ($CDCl_3$): δ 9.49 (d, 1H), 8.53 (d, 1H), 8.47 (d, 1H), 8.16 (d, 1H), 7.7 (m, 2H), 7.46 (t, 1H), 7.30 (t, 1H) (phenanthridine ring H); 8.93 (s, 1H, imine hydrogen); 3.85 (m, 1H, CH of cyclohexyl ring); 2.2–1.4 (m, 10H, CH_2 of cyclohexyl ring).

Metal complexes

The silver and zinc complexes of the **tcp** and **ccp** ligands were obtained by the same procedure, *i.e.* by mixing 5–10 mg samples of ligand with the stoichiometric amount of dry Ag(I) or Zn(II) trifluoromethanesulfonate in 2 ml CH_3CN, from which the complexes precipitated as yellowish crystalline solids by diffusion of diethyl ether.

[Ag₂(tcp)₂](CF₃SO₃)₂·(C₂H₅)₂O

Yield 76%. Anal. Calc. for $C_{74}H_{66}N_8Ag_2F_6O_7S_2$: C 56.49, H 4.23, N 7.12%. Found: C 56.43, H 4.26, N 7.08%. ^{1}H NMR (CD_3CN): δ 9.4 (m, 2H, imine CH=N); 8.9 (m, 2H), 8.65 (d, 2H), 8.55 (m, 2H), 8.0 (m, 2H), 7.8 (t, 2H), 7.5–7.7 (m, 6H) (phenathridine ring H); 3.8 (m, 2H, CH–N of cyclohexanediyl ring); 0.9–2.1 (m, CH_2 of cyclohexanediyl ring). Mass (ESI): $m/z = 1347, 1349, 1351$, for $\{[Ag_2(\textbf{tcp})_2](CF_3SO_3)\}^+$.

[Ag₂(ccp)₂](CF₃SO₃)2·(C₂H₅)₂O

Yield 88%. Anal. Calc. for $C_{74}H_{66}N_8Ag_2F_6O_7S_2$: C 56.49, H 4.23, N 7.12%. Found: C 56.41, H 4.21, N 7.15%. ^{1}H NMR (CD_3CN): δ 10.20 (d, 1H), 9.50 (d, 1H), 9.03 (d, 1H), 8.92 (d, 1H), 8.70 (d, 1H), 8.28 (d, 1H), 8.22 (t, 1H), 8.17 (t, 1H), 7.95–7.8 (m, 4H), 7.7–7.5 (m, 4H), 7.45 (t, 1H), 7.22 (t, 1H) (phenanthridine ring H and imine H); 3.6 (m, 2H, CH–N of cyclohexanediyl ring); 1.0–2.0 (m, CH_2 of cyclohexanediyl ring). Mass (ESI): $m/z = 1347, 1349, 1351$, for $\{[Ag_2(\textbf{ccp})_2](CF_3SO_3)\}^+$.

[Zn(tcp)](CF₃SO₃)₂·H₂O

Yield 65%. Anal. Calc. for $C_{36}H_{30}F_6N_4O_7S_2Zn$: C 49.46, H 3.46,

N 6.41%. Found: C 49.49, H 3.41, N 6.38%. Mass (ESI): $m/z = 707$ for $\{[Zn(\textbf{tcp})](CF_3SO_3)\}^+$.

[Zn(ccp)](CF₃SO₃)₂·2H₂O

Yield 58%. Anal. Calc. for $C_{36}H_{32}F_6N_4O_8S_2Zn$: C 48.47, H 3.62, N 6.28%. Found: C 48.28, H 3.57, N 6.22%. Mass (ESI): $m/z = 707$ for $\{[Zn(\textbf{tcp})](CF_3SO_3)\}^+$.

Spectrophotometric titrations and formation constants

In a typical experiment, titrations were carried out on 50 ml portion of a 1×10^{-4}–1×10^{-5} M acetonitrile solution of the chosen ligand, to which substoichiometric quantities of an acetonitrile solution of the chosen metal triflate were added. The concentration of the metal salt solutions were such that one equivalent of metal was added in 100–200 μl. 20–30 Absorbance *vs* > volume of titrant points were taken for each titration. Formation constants were obtained from titration data through non-linear least squares refinement with the Hyperquad2000 package.[6]

Fluorimetric experiments

The solvent used for photophysical measurements was acetonitrile from Merck (UVASOL) without further purification. Uncorrected emission, and corrected excitation spectra were obtained with a Fluorolog spectrofluorimeter equipped with a Hamamatsu R928 phototube. Luminescence quantum yields (uncertainty ± 15%) were determined using quinine sulfate in a 0.05 M solution of sulfuric acid ($\Phi = 0.546$ in aerated aqueous acid solution[7]) as standard. In order to allow comparison of emission intensities, corrections for instrumental response, inner filter effects and phototube sensitivity were performed.[8] A correction for differences in the refractive indices was introduced when necessary.

X-Ray data collection and processing

The crystal and molecular structure of the $[Ag_2(\textbf{ccp})_2](CF_3SO_3)$-$(Et_2O)$ complex has been determined by X-ray diffraction methods. Unit cell parameters and intensity data were obtained on an Enraf-Nonius CAD-4 four-circle diffractometer at room temperature using graphite-monochromatized Mo-Kα radiation. Calculations were performed with the WinGX-97 software.[9] Crystal data and the most relevant parameters used in the crystallographic study are reported in Table 1. Cell dimensions were determined by least-squares fitting of 25 centred reflections monitored in the range $6.21 < \theta < 10.33°$. Corrections for Lp and empirical absorption were applied.[10] The structure was solved by SIR92.[11] The non-hydrogen atoms were refined anisotropically by full-matrix least-squares using SHELXL-97.[12] Hydrogen atoms were inserted in the calculated positions and refined with isotropic displacement factors proportional to those of their neighbouring atoms. Atomic scattering factors were taken from *International Tables for X-ray Crystallography*.[13] Diagrams of the molecular structure were produced by the ORTEP-3 program.[14]

CCDC reference number 213788.

See http://www.rsc.org/suppdata/dt/b3/b307285a/ for crystallographic data in CIF or other electronic format.

Computational chemistry

Molecular dynamics calculations were run with the Hyper-Chem 3 for Windows package (Hypercube Inc. & Autodesk Inc.) to find the most stable structures for the ligands and Zn^{2+} molecular complexes. The geometry optimization was performed using the MM+ force field, which is an extension of MM2, contained in the HyperChem Help Database. Additional calculations were run, including acetonitrile molecules, to evaluate solvent effects on the stability of the complexes.

Table 1 Crystal and refinement data

Formula	$C_{74}H_{66}Ag_2F_6N_8O_7S_2$
M_w	1573.21
Crystal size/mm	$0.07 \times 0.18 \times 0.70$
Crystal system	Triclinic
Space group	$P\bar{1}$
a/Å	12.317(3)
b/Å	16.705(4)
c/Å	17.211(5)
α/°	91.09(2)
β/°	97.00(2)
γ/°	105.86(2)
V/Å^3	3376.0(14)
Z	2
D_c/g cm^{-3}	1.548
T/K	298(3)
μ/mm^{-1}	0.721
Scan type	ω–2θ
θ Range/°	2–25
Absorption correction method	ψ-Scan
Index ranges, hkl	-14 to 14, -19 to 19, 0 to 20
Reflns measured/unique (R_{int})	12288/11855 (0.0332)
Refinement type	F^2
$R_1{}^a$	0.0595
R_{all}	0.1184
wR_2	0.1440
GOF^b	1.064
Refined parameters	894
Weighting scheme	$w = 1/[\sigma^2(F_o{}^2) + (0.0386P)^2 + 7.9157P]$ where $P = (F_o{}^2 + 2F_c{}^2)/3$
(Shift/esd)$_{max}$	0.000
Max., min. $\Delta\rho$/e Å^{-3}	1.328, -0.842

^{a} $R_1 = \Sigma||F_o| - |F_c||/\Sigma|F_o|$ (calculated on 7232 reflections with $I > 2\sigma_I$). ^{b} GOF $= S = [\Sigma[w(F_o{}^2 - F_c{}^2)^2]/(n - p)]^{0.5}$, where n is the number of reflections and p is the total number of parameters refined.

Intrumentation

Mass spectra (ESI) were recorded on a Finnigan MAT TSQ 700 instrument, NMR spectra on a Bruker AMX 400 spectrometer (CD$_3$CN as solvent), UV/Vis spectra on a Hewlett-Packard HP8453 diode array spectrophotometer.

Results and discussion

(1) Photophysical properties of the ligands in solution

As has been already reported, the phenanthridine chromophore has interesting and well known photophysical properties.[15] Its absorption spectrum in acetonitrile solution presents a structured band with the lowest energy feature at 343 nm ($\varepsilon_{343} = 1200$ M^{-1} cm^{-1}). The fluorescence band is also structured, with λ_{max} at 370 nm ($\phi = 9 \times 10^{-3}$, $\tau = 0.6$ ns). Cyclohexyl-phenanthridine, **cp**, which presents only one phenanthridine chromophore, can be considered as the "half" of the two ligands **tcp** and **ccp**, and can act as a model compound in which no intramolecular phenanthridine–phenanthridine interactions are possible. **cp** displays different photophysical properties with respect to plain phenanthridine, indicating that the delocalisation caused by the substitution with an imino function has a great influence on its electronic states. In particular, the absorption spectrum in acetonitrile solution of cyclohexylphenanthridine presents two bands centred at 254 and 305 nm ($\varepsilon_{254} = 40000$ and $\varepsilon_{305} = 9000$ M^{-1} cm^{-1}). As far as the fluorescence is concerned, this compound shows a large emission band with $\lambda_{max} = 440$ nm ($\phi = 2 \times 10^{-3}$). The photophysical properties of the ligands **tcp** and **ccp** in the same experimental conditions present some interesting differences compared with the model species. While the absorption spectra are very similar presenting two bands centred at the same wavelengths and with a molar absorption that is roughly double of the values found for the model compound ($\varepsilon_{254} = 87000$ and $\varepsilon_{305} = 20000$ M^{-1} cm^{-1} for **tcp** and $\varepsilon_{254} = 74000$ and $\varepsilon_{305} = 18000$ M^{-1} cm^{-1} for **ccp**), both ligands present a large emission band at 550 nm ($\phi = 8 \times 10^{-2}$

and $\tau = 7.5$ ns for **ccp** and $\phi = 5 \times 10^{-3}$ and $\tau = 7.2$ ns for **tcp**) that is largely red-shifted (*ca*. 4550 cm^{-1}) compared to the **cp** one. The excitation spectra of both ligands match very well the absorption ones, clearly indicating that the observed fluorescence is not due to other species, such as adventitious impurities. This can be explained by considering that each ligand presents two substituted phenanthridine and that intramolecular excimer formation between the two chromophoric arms of the ligands can occur.[16] The differences are enhanced in the **ccp** ligand in comparison with the **tcp** one, most probably for conformational reasons. Molecular modelling[17] supports this hypothesis, as minimum energy structures are found both for **ccp** and **tcp** in which the two phenanthridine moieties are parallel and facing each other (Fig. 1), with larger stacked portions of the aromatic ring systems in **ccp**. This is of course not possible for the monomeric species **cp**, for which also intermolecular π–π stacking interactions can be ruled out because of the very low concentrations ($<3 \times 10^{-5}$ M) used for photophysical experiments.
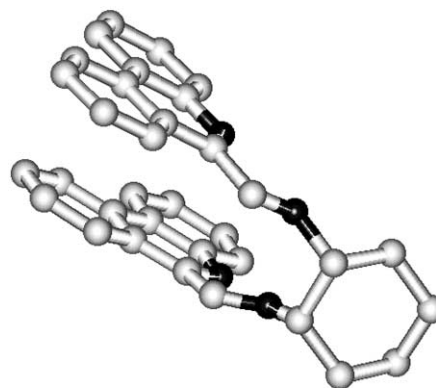

Fig. 1 Molecular model for ligand **ccp**. Carbon atoms in shaded white, nitrogen atoms in black.

Table 2 Calculated formation constants. The indices indicate respectively the number of ligands and the number of metal cations in the complex. The uncertainty of each calculated value is reported in parenthesis

	Ag^+	Cu^+	Zn^{2+}
tcp	$\log K_{21} = 8.8\ (0.3)$	$\log K_{21} = 9.6\ (0.2)$	$\log K_{11} = 10.39\ (0.05)$
	$\log K_{22} = 15.2\ (0.2)$	$\log K_{22} = 16.75\ (0.2)$	$\log K_{21} = 18.49\ (0.05)$
ccp	$\log K_{21} = 10.9\ (0.1)$	$\log K_{21} = 12.3\ (0.1)$	$\log K_{11} = 8.8\ (0.1)$
	$\log K_{22} = 16.9\ (0.1)$	$\log K_{22} = 19.5\ (0.1)$	$\log K_{21} = 15.0\ (0.1)$

(2) Complex formation and properties in solution

The ligands **tcp** and **ccp** present a fair affinity for the Ag^+, Cu^+ and Zn^{2+} ions and we have been able to study the complex formation with these cations in acetonitrile solution through spectrophotometric and spectrofluorimetric measurements, as noticeable variations of the absorption and emission spectra are observed upon addition of the cations to solutions of the ligands. In the case of Ag^+ intense absorption bands grow in the region between 300 and 450 nm, while the band centered at 305 nm, typical of the ligands, decreases in intensity (Fig. 2).
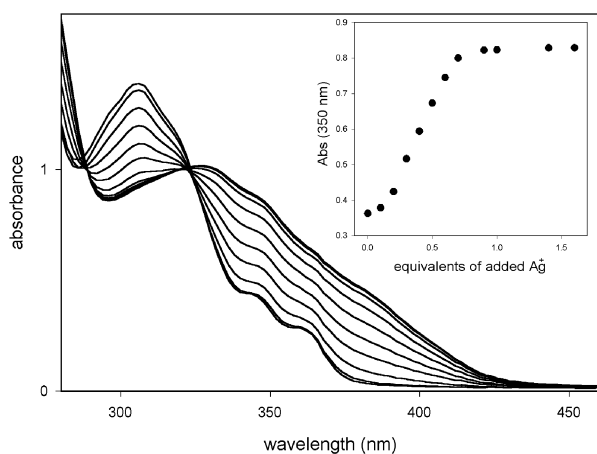

Fig. 2 Absorption spectra for the addition of substoichiometric quantities of Ag^+ to ligand **tcp** in acetonitrile. The band at 305 nm decreases while the shoulder at 320–400 nm increases in intensity. In the inset, the titration profile of the absorbance at 350 nm *vs.* equivalents of added Ag^+ is reported.

The presence of two different species and of their relative equilibria of formation is evidenced by the observation of two different isosbestic points for the 0–0.5 and 0.5–1.0 interval of equivalents of added Ag^+ ions. Although by plotting the values of absorbance at $\lambda = 350$ nm *vs.* the equivalents of added Ag^+ (Fig. 2, inset) an almost linear increase is observed, with only a slight change in slope before 1 : 1 molar ratio (after which ratio, additions of further Ag^+ does not result in any change) the formation of stable complexes with both a 1 : 2 and 1 : 1 stoichiometry, *i.e.* $[Ag(\textbf{tcp})_2]^+$ and $[Ag_2(\textbf{tcp})_2]^{2+}$, is confirmed by calculation of formation constants. The absorbance data were used to calculate the formation constants by means of non-linear least-squares regression, through the Hyperquad2000 calculation package,[6] and the data fitted only with a model featuring equilibria for both 1 : 2 and 2 : 2 metal–ligand species. The values relative to the formation constants for the following equilibria in acetonitrile are reported in Table 2 (**L** = **tcp** or **ccp**):

$$Ag^+ + 2L \leftrightarrow [Ag(L)_2]^+ \ (K_{21})$$
$$2Ag^+ + 2L \leftrightarrow [Ag_2(L)_2]^{2+} \ (K_{22})$$
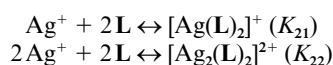
According to the calculated values, for a solution containing an equimolar ratio of Ag^+ and **tcp** or **ccp**, 96.5% and 95.6% respectively, of the $[Ag_2(\textbf{tcp})_2]^{2+}$ and $[Ag_2(\textbf{ccp})_2]^{2+}$ complexes can be found at a total Ag^+ and ligand concentration of 10^{-3} M (concentration of the dimeric species = 5×10^{-4} M). Besides,

examination of the mass spectrum (ESI technique) of a solution containing a 1 : 1 molar ratio of Ag^+ and **tcp** revealed the typical signal of the $[Ag_2(\textbf{tcp})_2]^{2+}$ complex, with $m/z = 1347$, 1349, 1351 for the $\{[Ag_2(\textbf{tcp})_2]CF_3SO_3\}^+$ cation, thus further demonstrating that the observed sharp change in the titration profile at 1 : 1 molar ratio and the absence of further variations for further additions of Ag^+ cations is indeed representative of the formation of the expected stable 2 : 2 complex.[18]

The dimetallic complexes are expected to present a double helical structure on the basis of what has already been observed for the $[Cu^I{}_2(\textbf{tcp})_2]^{2+}$ and $[Cu^I{}_2(\textbf{ccp})_2]^{2+}$ complexes[1b] and this was confirmed both by the crystal structure determination (see Section 3) and by ^{1}H NMR measurements in CD$_3$CN (see Experimental section for chemical shifts). For $[Ag_2(\textbf{tcp})_2]^{2+}$ a spectrum with only one pattern of signals in the aromatic region is obtained, which is what has been already found with the corresponding Cu^+ complex, and originates from a symmetric helical structure. The multiplicity of the signals is increased by the ^{1}H–^{107,109}Ag coupling[4] and no singlets are found even for the imine protons. Considering that **tcp** is chiral (we used the *R,R* isomer) and the one-pattern NMR spectrum that is observed, the $[Ag_2(\textbf{tcp})_2]^{2+}$ helicate should be *M*-handed, by comparison with what has already been observed for Cu^+ with the same ligand, containing quinoline instead of phenanthridine as the heterocycle.[19] A CD spectrum has also been recorded for this complex in acetonitrile, which displays bands centered at 230 nm ($\Delta\varepsilon = +12$ M^{-1} cm^{-1}), 278 nm ($\Delta\varepsilon = -23$ M^{-1} cm^{-1}), 328 nm ($\Delta\varepsilon = +8$ M^{-1} cm^{-1}), 360 nm ($\Delta\varepsilon = -5$ M^{-1} cm^{-1}) and 408nm ($\Delta\varepsilon = +5$ M^{-1} cm^{-1}). On the other hand, for the $[Ag_2(\textbf{ccp})_2]^{2+}$ complex a sharp spectrum with two sets of signals in the aromatic zone is obtained, as already found for the analogous $[Cu^I{}_2(\textbf{ccp})_2]^{2+}$ complex,[1b] and in agreement with the double set of signals found also for the double helical complex of the Ag^+ cation with a ligand featuring the same *cis*-1,2-cyclohexanediyl spacer and two pyridine heterocycles.[4] The doubling of the aromatic protons originates from the different environment found for the two imino-heterocycle halves of a single ligand, in a structure which is the same found in the solid state (Fig. 5). One half of each ligand is face-to-face with one half of the second ligand, while the other half is alone and pointing outward with respect to the molecular cation. Noticeably, no singlets are found in the aromatic chemical shifts zone, as also the imine protons appear as doublets, as expected from the ^{1}H–^{107,109}Ag coupling.

The same spectrophotometric titration experiments and calculations were also carried out, for sake of comparison, for the Cu^+ cation (Table 2). The same kind of equilibria as for Ag^+ were found for Cu^+. The $\log K$ values found for each equilibrium with Cu^+ are larger with respect to Ag^+, this reflecting the trend found with these two metal centres and ligands featuring comparable donor sets with respect to **tcp** and **ccp** (*e.g.* 2,2′ bipyridine[20]). Finally, as far as the emission spectra are concerned, addition of Ag^+ and Cu^+ ions quenches the ligand fluorescence, and the complexes formed with these two metal ions do not present any appreciable luminescence with both **tcp** and **ccp** ligands.

Spectrofluorimetric and spectrophotometric titrations carried out with Zn^{2+} ions disclosed a different behaviour. Noticeably, as for the complexation of Ag^+ cations, by observing the changes in the absorption spectra upon addition of

increasing amounts of Zn^{2+} ions (Fig. 3 for **tcp** as ligand), the formation of two different species is found: two different couples of isosbestic points are observed for the 0–0.5 and 0.5–1.0 equivalents intervals.
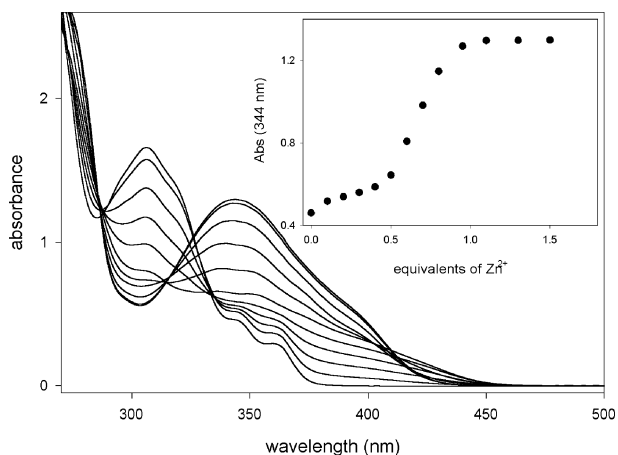

Fig. 3 Absorption spectra for the addition of substoichiometric quantities of Zn^{2+} to ligand **tcp** in acetonitrile. The band at 305 nm decreases in intensity, while the shoulder at 400 nm and the band at 344 nm increase. The isosbestic point at 330 nm is mantained in the 0–0.5 equiv. interval while the isosbestic point at 315 nm is observed in the 0.5–1.0 equiv. of added metal interval. In the inset, the titration profile of the absorbance at 344 nm *vs.* equivalents of added Zn^{2+} is reported

Moreover, beside the formation of a 1 : 2 metal–ligand complex, spectrophotometric titrations and ESI measurements demonstrated the formation of the monomeric $[Zn(tcp)]^{2+}$ and $[Zn(ccp)]^{2+}$ complexes at 1 : 1 metal–ligand molar ratio. A peak at $m/z = 707$ was found, for the $\{[Zn(tcp)]CF_3SO_3\}^+$ and $\{[Zn(ccp)]CF_3SO_3\}^+$ species. This can be explained with the tendency of the bipositive Zn^{2+} cation to reach coordination numbers higher then four, and therefore a structure similar to that found for the Cu^{2+} complexes [1d] with the same ligands can be hypothesized for $[Zn(tcp)]^{2+}$ and $[Zn(ccp)]^{2+}$, with the ligands arranged in a square disposition around the metal cation, and two solvent molecules completing the coordination sphere in the apical positions of a distorted octahedron. In agreement, molecular modelling calculations [17] confirm that the complexes in which the two solvent molecules are *trans* with respect to the ligands are ~10 kcal mol^{-1} more stable than the complexes in which they assume *cis* disposition.

All the Zn^{2+} complexes with the **ccp** or **tcp** ligands are more luminescent then the ligands alone. The profiles of emission intensities recorded during the spectrofluorimetric titrations with the Zn^{2+} ions present substantial variations (see Fig. 4).
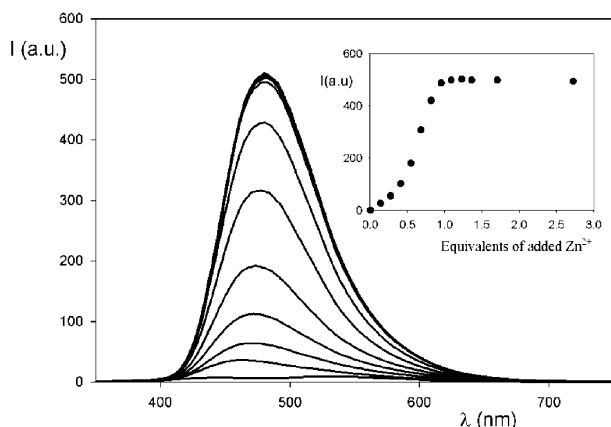

Fig. 4 Emission spectra profiles titrating the ligand **tcp** with increasing amounts of Zn^{2+} ions; inset: plot of the emission intensities at 482 nm *vs.* equivalents of added Zn^{2+}.

The maximum of the emission band shifts from 550 to 482 nm for both ligands while the intensity value of the maximum increases for the two species ($\lambda_{max} = 482$, $\phi = 0.12$ and $\tau = 8.5$ ns and $\lambda_{max} = 472$, $\phi = 5 \times 10^{-2}$ and $\tau = 9.3$ ns for **ccp** in 1 : 1 and 1 : 2 stoichiometry, respectively, and $\lambda_{max} = 4$ 82, $\phi = 8 \times 10^{-2}$ and $\tau = 7.7$ ns and $\lambda_{max} = 472$, $\phi = 5 \times 10^{-2}$ and $\tau = 7.3$ ns for **tcp** in 1 : 1 and 1 : 2 stoichiometry, respectively).

It should also to be stressed that $\log K$ values for the complexes of the two ligands and Zn^{2+} can be calculated also from the profile of emission data *vs.* equivalents of added metal cation: the obtained results are in very good agreement with those obtained from the absorption spectra. The lack of luminescence from the Ag^+ and Cu^+ complexes can be attributed to the possibility, typical of these latter ions, to give rise to photoinduced electron transfer processes, that are usually not accessible for Zn^{2+} ions.

(3) Crystal and molecular structure of $[Ag_2(ccp)_2](CF_3SO_3)_2 \cdot (CH_3CH_2)_2O$

The crystal and molecular structure of the complex is shown in Fig. 5. It consists of separated $[Ag_2(ccp)_2]^{2+}$ molecular cations and $CF_3SO_3^-$ anions, which do not interact with Ag^+ ions; one diethyl ether molecule is also present in the structure. In the $[Ag_2(ccp)_2]^{2+}$ molecular cation, Ag^I metal centres are co-ordinated by two nitrogen atoms from each **ccp** ligand. The two **ccp** ligands intertwine to give a double helix. Two of the phen-anthridine rings, one from each **ccp** ligand, face each other with an angle between mean planes of 7.6(1)° and distance ranging between 3.18 and 3.76 Å, in a disposition closely resembling what has already been found for the double helical complex between **ccp** and Cu^+.[1d] In the molecular cation, the co-ordination around each Ag^+ ion can be described as distorted tetrahedral. The distance between the two Ag^+ ions is 3.045(1) Å. The crystal is maintained by van der Waals forces.
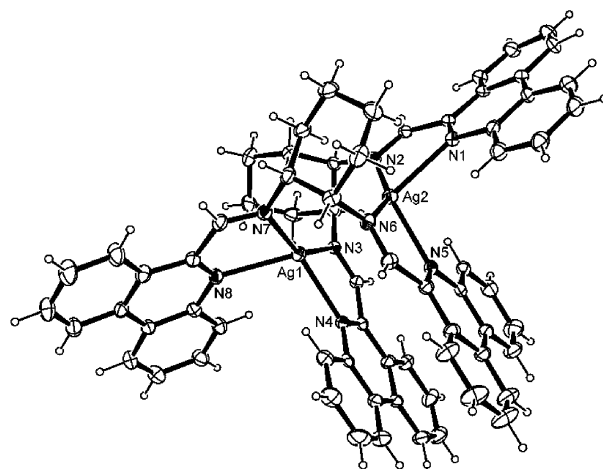

Fig. 5 ORTEP view of the $[Ag_2(ccp)_2]^{2+}$ molecular cation with thermal ellipsoids drawn at 20% probability level. The triflate anions as well as the diethyl ether molecule have been omitted for clarity. Selected bond lengths (Å) and angles (°): Ag1–N7 2.307(5), Ag1–N4 2.352(5), Ag1–N3 2.375(5), Ag1–N8 2.405(5), Ag2–N2 2.261(5), Ag1–N6 2.320(6), Ag1–N5 2.330(5), Ag1–N1 2.426(5); N3–Ag1–N4 70.7(2), N3–Ag1–N7 146.0(2), N3–Ag1–N8 120.9(2), N4–Ag1–N7 139.5(2), N4–Ag1–N8 107.6(2), N7–Ag1–N8 71.6(2), N1–Ag$_2$–N2 71.9(2), N1–Ag$_2$–N5 104.2(2), N1–Ag$_2$–N6 121.2(2), N2–Ag$_2$–N5 134.4(2), N2–Ag$_2$–N6 150.5(2), N5–Ag$_2$–N6 71.4(2).

References

1 (*a*) M. A. Masoosd, E. J. Enemark and T. D. P. Stack, *Angew. Chem., Int. Ed.*, 1998, **37**, 928; (*b*) V. Amendola, L. Fabbrizzi, L. Linati, C. Mangano, P. Pallavicini, V. Pedrazzini and M. Zema, *Chem. Eur. J.*, 1999, **5**, 3679; (*c*) V. Amendola, L. Fabbrizzi and P. Pallavicini, *Coord. Chem. Rev.*, 2001, **216–271**, 435; (*d*) V. Amendola, L. Fabbrizzi, L. Gianelli, C. Maggi, C. Mangano, P. Pallavicini and M. Zema, *Inorg. Chem.*, 2001, **40**, 3579.

2 (*a*) T. M. Garrett, U. Koert, J.-M. Lehn, A. Rigault, D. Meyer and J. Fischer, *J. Chem. Soc., Chem. Commun.*, 1990, 557; (*b*) T. M. Garrett, U. Koert and J.-M. Lehn, *J. Phys. Org. Chem.*, 1992, **5**, 529; (*c*) E. C. Constable, S. M. Helser, M. J. Hannon, A. Martin, P. R. Raithby and D. A. Tocher, *J. Chem. Soc., Dalton Trans.*, 1996, 2423; (*d*) J. Hamblin, L. J. Childs, N. W. Alcock and M. J. Hannon, *J. Chem. Soc., Dalton Trans.*, 2002, 164; (*e*) M. J. Hannon, S. Bunce, A. J. Clarke and N. W. Alcock, *Angew. Chem., Int. Ed.*, 1999, **38**, 1277.

3 (*a*) R. Prabaharan and N. C. Fletcher, *J. Chem. Soc., Dalton Trans.*, 2003, 2558; (*b*) E. C. Constable, M. Neuburger, D. R. Smith and A. Zehnder, *Chem. Commun.*, 1996, 1917; (*c*) C. Piguet, G. Berardinelli, B. Bocquet, A. Quattropani and A. F. Williams, *J. Am. Chem. Soc.*, 1992, **114**, 7440.

4 G. C. Van Stein, G. van Koten, K. Vieze, C. Brevard and A. L. Speck, *J. Am. Chem. Soc.*, 1984, **106**, 4486.

5 T. Eicher and A. Kruse, *Synthesis*, 1985, 612.

6 P. Gans, A. Sabatini and A. Vacca, *Talanta*, 1996, **43**, 1739.

7 S. R. Meech and D. Phillips, *J. Photochem.*, 1983, **54**, 159.

8 L. Prodi, M. Montalti, N. Zaccheroni, G. Pickaert, L. Charbonnière and R. Ziessel, *New J. Chem.*, 2003, **27**, 134–139.

9 L. J. Farrugia, WinGX-97, An integrated system of Publicly Available Windows Programs for the Solution, Refinement and Analysis of Single-Crystal X-Ray Diffraction, University of Glasgow, 1997.

10 A. C. T. North, D. C. Philips and F. S. Mathews, *Acta Crystallogr., Sect. A*, 1968, **24**, 351.

11 A. Altomare, G. Cascarano, C. Giacovazzo and A. J. Gualardi, *J. Appl. Crystallogr.*, 1993, **26**, 343–350.

12 G. M. Sheldrick, SHELX-97, Programs for Crystal Structure Analysis, University of Göttingen, Germany, 1998.

13 *International Tables for X-ray Crystallography*, Kynochn Birmingham, England, 1974, vol. 4, pp. 99–101 and 149–150.

14 L. J. Farrugia, *J. Appl. Crystallogr.*, 1997, 565.

15 (*a*) C. J. Marzacco, G. Deckey, R. Colarulli, G. Siuzdak and A. M. Halpern, *J . Phys. Chem.*, 1989, **93**, 2935–2939; (*b*) S. L. Murov, I. Carmichael, G. L. Hug, *Handbook of Photochemistry*, Marcel Dekker, INC, 1993.

16 Comparing the luminescence of **tcp** and **ccp** with that of **cp**, the most noticeable change is the large red shift. This behaviour is typical of excimer formation (see, for example: A. Gilbert and J. Baggot, *Essential of Molecular Photochemistry*, Blackwell Scientific Publications, Oxford, 1981;). The difference in intensity can be attributed to the change of the nature and energy of the lowest excited state.

17 HyperChem 3 for Windows package (Hypercube Inc. & Autodesk Inc.). Geometry optimization was performed using the MM+ force field, which is an extension of MM2, contained in the HyperChem Help Database.

18 The formation of 1:2 metal/ligand complexes for low metal/ligand ratios is supported also by literature published for comparable systems, see: J. Hamacek, S. Blanc, M. Elhabiri, E. Leize, A. Van Dorsselear, C. Piguet and A.-M. Albrecht-Gary, *J. Am. Chem. Soc.*, 2003, **125**, 1541.

19 V. Amendola, L. Fabbrizzi, C. Mangano, P. Pallavicini, E. Roboli and M. Zema, *Inorg. Chem.*, 2000, **39**, 5803.

20 M. Munakata, S. Kitagawa and M. Miyazima, *Inorg. Chem.*, 1985, **24**, 1638.